

Tuning Frictional Properties of Kirigami Altered Graphene Sheets using Molecular Dynamics and Machine Learning

Designing a Negative Friction Coefficient

Mikkel Metzsch Jensen



Thesis submitted for the degree of
Master in Computational Science: Materials Science
60 credits

Department of Physics
Faculty of mathematics and natural sciences

UNIVERSITY OF OSLO

Spring 2023

Tuning Frictional Properties of Kirigami Altered Graphene Sheets using Molecular Dynamics and Machine Learning

Designing a Negative Friction Coefficient

Mikkel Metzsch Jensen



© 2023 Mikkel Metzsch Jensen

Tuning Frictional Properties of Kirigami Altered Graphene Sheets using Molecular Dynamics and Machine Learning

<http://www.duo.uio.no/>

Printed: Reprocentralen, University of Oslo

Abstract

Abstract.

Acknowledgments

Acknowledgments.

List of Symbols

F_N Normal force (normal load)

Acronyms

MD molecular dynamics. 2, 3

ML machine learning. 2, 3

Contents

1	Introduction	1
1.1	Motivation	1
1.2	Approach	3
1.3	Contributions	3
1.4	Thesis structure	3
I	Background Theory	5
2	Tribology - friction	7
2.1	Macroscale	7
2.1.1	Amontons' law	7
2.2	Microscopic scale	9
2.2.1	Surface roughness - Asperity theories	9
2.3	Nanoscale - Atomic scale	10
2.3.1	Frenkel-Kontorova	11
2.3.1.1	Commensurability	12
2.3.1.2	Kinetic friction	14
2.3.1.3	Temperature dependence	15
2.3.1.4	Smooth sliding	15
2.3.2	Experimental procedures	15
2.3.2.1	Scanning Probe Microscopy	15
2.3.2.2	Surface Force Apparatus (SFA)	16
2.3.3	(summary of) Expected frictional properties	16
2.3.3.1	Qualitatively	17
II	Simulations	19
Appendices		21
Appendix A		23
Appendix B		25
Appendix C		27

Chapter 1

Introduction

Structure of Motivation section:

1. Introduce and motivate friction broadly.
2. Motives for friction control using a grasping robot as example.
3. Analog to gecko feet where adhesive properties are turned on and off.
4. Interest in origin of friction through nanoscale studies which further motivates the use of MD.
5. Intro to metamaterials and the use of kirigami designs,
6. How to optimize kirigami designs with reference to Hanakata and motivating the use of ML.
7. Out-of-plane buckling motivates the use of kirigami for frictional properties.

Does some of the latter paragraphs belong to the approach section?

1.1 Motivation

Friction is a fundamental force that takes part in most of all interactions with physical matter. Even though the everyday person might not be familiar with the term *friction* we recognize it as the inherent resistance to sliding motion. Some surfaces appear slippery and some rough, and we know intuitively that sliding down a snow covered hill is much more exciting than its grassy counterpart. Without friction, it would not be possible to walk across a flat surface, lean against the wall without falling over or secure an object by the use of nails or screws [p. 5] [1]. It is probably safe to say that the concept of friction is integrated in our everyday life to such an extent that most people take it for granted. However, the efforts to control friction dates back to the early civilization (3500 B.C.) with the use of the wheel and lubricants to reduce friction in translational motion [2]. Today, friction is considered a part of the wider field *tribology* derived from the Greek word *Tribos* meaning “rubbing” and includes the science of friction, wear and lubrication [2]. The most compelling motivation to study tribology is ultimately to gain full control of friction and wear for various technical applications. Especially, reducing friction is of great interest as this has tremendous advantages for energy efficiency. It has been reported that tribological problems have a significant potential for economic and environmental improvements [3]:

“On global scale, these savings would amount to 1.4% of the GDP annually and 8.7% of the total energy consumption in the long term.” [4].

On the other hand, the reduction of friction is not the only sensible application for tribological studies. Controlling frictional properties, besides minimization, might be of interest in the development of a grasping robot where a finetuned object handling is required. While achieving a certain “constant” friction response is readily obtained through appropriate material choices during manufacturing, we are yet to unlock the capabilities to alter friction dynamically on the go. One example from nature inspiring us to think along these lines are the gecko feet. More precisely, the Tokay gecko has received a lot of attention in scientific studies aiming to unravel the underlying

mechanism of its “toggable” adhesion properties. Although geckos are able to produce large adhesive forces, they retain the ability to remove their feet from an attachment surface at will [5]. This makes the gecko able to achieve a high adhesion on the feet when climbing a vertical surface while lifting it for the next step remains relatively effortless. For a grasping robot we might consider an analog frictional concept of a surface material that can change from slippery to rough on demand depending on specific tasks.

In the recent years an increasing amount of interest has gone into the studies of the microscopic origin of friction, due to the increased possibilities in surface preparation and the development of nanoscale experimental methods. Nano-friction is also of great concern for the field of nano-machining where the frictional properties between the tool and the workpiece dictates machining characteristics [3]. With concurrent progress in computational power and development of Molecular Dynamics (MD), numerical investigations serve as an extremely useful tool for getting insight into the nanoscale mechanics associated with friction. This simulation based approach can be considered as a “numerical experiment” enabling us to create and probe a variety of high complexity systems which are still out of reach for modern experimental methods.

In materials science such MD-based numerical studies have been used to explore the concept of so-called *metamaterials* where material compositions are designed meticulously to enhance certain physical properties [6][7][8][9][10][11]. This is often achieved either by intertwining different material types or removing certain regions completely. In recent papers by Hanakata et al. [6](2018) [7](2020) numerical studies have showcased that mechanical properties of a graphene sheet, in this case yield stress and yield strain, can be altered through the introduction of so-called *kirigami* inspired cuts into the sheet. Kirigami is a variation of origami where the paper is cut additionally to being folded. While these methods originate as an art form, aiming to produce various artistic objects, they have proven to be applicable in a wide range of fields such as optics, physics, biology, chemistry and engineering [12]. Various forms of stimuli enable direct 2D to 3D transformations through folding, bending, and twisting of microstructures. While original human designs have contributed to specific scientific applications in the past, the future of this field is highly driven by the question of how to generate new designs optimized for certain physical properties. However, the complexity of such systems and the associated design space makes for seemingly intractable problems ruling out analytic solutions.

Earlier architecture design approaches such as bioinspiration, looking at gecko feet for instance, and Edisonian, based on trial and error, generally rely on prior knowledge and an experienced designer [9]. While the Edisonian approach is certainly more feasible through numerical studies than real world experiments, the number of combinations in the design space rather quickly becomes too large for a systematic search, even when considering the simulation time on modern day hardware. However, this computational time constraint can be relaxed by the use of machine learning (ML) which have proven successful in the establishment of a mapping from the design space to physical properties of interest. This gives rise to two new styles of design approaches: One, by utilizing the prediction from a trained network we can skip the MD simulations all together resulting in an *accelerated search* of designs. This can be further improved by guiding the search accordingly to the most promising candidates, as for instance done with the *genetic algorithm* which suggest new designs based on mutation and crossing of the best candidates so far. Another, even more sophisticated approach, is through generative methods such as *Generative Adversarial Networks* (GAN). By working with a so-called *encoder-decoder* network structure, one can build a model that reverses the prediction process. That is, the model predicts a design from a set of physical target properties. In the papers by Hanakata et al. both the *accelerated search* and the *inverse design* approach was proven successful to create novel metamaterial kirigami designs with the graphene sheet.

Hanakata et al. attributes the variety in yield properties to the non-linear effects arising from the out-of-plane buckling of the sheet. Since it is generally accepted that the surface roughness is of great importance for frictional properties it can be hypothesized that the kirigami cut and stretch procedure can also be exploited for the design of frictional metamaterials. For certain designs we might hope to find a relationship between stretching of the sheet and frictional properties. If significant, this could give rise to a variability of the friction response beyond manufacturing material choice. For instance, the grasping robot might apply such a material as artificial skin for which stretching or relaxing of the surface could result in a changeable friction strength; Slippery and smooth when in contact with people and rough and firmly gripping when moving heavy objects. In addition, a possible coupling between stretch and the normal load through a nanomachine design would allow for an altered friction coefficient. This invites the idea of non-linear friction coefficients which might in theory also take on negative values given the right response from stretching. The latter would constitute an extremely rare property. This has (**only?**) been reported indirectly for bulk graphite by Deng et al. [13] where the friction kept increasing during the unloading phase. **Check for other cases and what I can really say here.**

To the best of our knowledge, kirigami has not yet been implemented to alter the frictional properties of a nanoscale system. In a recent paper by Liefferink et al. [14](2021) it is reported that macroscale kirigami can be used to dynamically control the macroscale roughness of a surface through stretching which was used to change the frictional coefficient by more than one order of magnitude. This supports the idea that kirigami designs can in fact be used to alter friction, but we believe that taking this concept to the nanoscale regime would involve a different set of underlying mechanisms and thus contribute to new insight in this field.

1.2 Approach

In this thesis we investigate the possibility to alter and control the frictional properties of a graphene sheet through application of kirigami inspired cuts and stretching of the sheet. With the use of MD simulations we evaluate the friction properties under different physical conditions in order to get insight into the prospects of this field. By evaluating variations of two kirigami inspired patterns and a series of random walk generated patterns we create a dataset containing information of the frictional properties associated with each design under different load and stretch conditions. We apply ML to the dataset and use an accelerated search approach to optimize for different properties of interest. The subtask of the thesis are presented more comprehensively in the following.

1. Define a sheet indexing that allows for a unique mapping of patterns between a hexagonal graphene lattice representation to a matrix representation suited for numerical analysis.
2. Design a MD simulation procedure to evaluate the frictional properties of a given graphene sheet under specified physical conditions such as load, stretch, temperature etc.
3. Find and implement suitable kirigami patterns which exhibit out-of-plane buckling under tensile load. This includes the creation of a framework for creating variations within each pattern class. Additionally create a procedure for generating different styles of random walk patterns.
4. Perform a pilot study of a representative subset of patterns in order to determine appropriate simulation parameters to use for the further study along with an analysis of the frictional properties shown in the subset.
5. Create a dataset consisting of the chosen kirigami variations and random walk patterns and analyse data trends.
6. Train a neural network to map from the design space to physical properties such as mean friction, maximum friction, contact area etc. and evaluate the performance.
7. Perform an accelerated search optimizing for interesting frictional properties using the ML model. This should be done both through the pattern generation procedures and by following a genetic algorithm approach.
8. Use the most promising candidates from the accelerated search to investigate the prospects of creating a nanomachine setup which exhibits a negative friction coefficient.
9. Study certain designs of interest with the scope of revealing underlying mechanism. This includes simple correlation analysis but also a visualization of feature and gradient maps of the ML network.

Is the list of subtask too specific? Some of the details here might be better suited for the thesis structure section.

1.3 Contributions

What did I actually achieve

1.4 Thesis structure

How is the thesis structured.

Part I

Background Theory

Chapter 2

Tribology - friction

Friction is a part of the wider field tribology which includes the study of friction, wear and lubrication between two surfaces in relative motion [1, p. 1]. In this thesis we will only concern ourselves with so-called wearless dry friction. That is, without any use of lubrication and without any resulting wear of the contacting surfaces. Tribological systems take place across a broad range of time and length scales, ranging from geological stratum layers involved in earthquakes [3] to microscopic atomistic processes, as in the gliding motion of a nanocluster of a nanomotor [15]. This vast difference in scale gives rises to different frictional mechanism being dominating at different scales. On a macro scale the system is usually subject to relatively high loads and speeds leading to high contact stresses and wear. On the other hand, the micro-/nanoscale regime occupies the opposite domain operating under relatively small loads and speeds with negligible wear [3] [2, p. 5]. While macroscale friction is often reduced into a few variables such as load, material type, speed and surface roughness it is clear that the micro-/nanoscale friction cannot be generalized under such a simple representation. On the micro-/nanoscale the tribological properties dominated by surface properties which will introduce an additional sensitivity variables such as temperature, humidity and even sliding history. The works of Bhushan and Kulkarni [16, (1996)] showed that the friction coefficient decreased with scale even though the materials used was unchanged. This reveals an intrinsic relationship between friction and scale as the contact condition is altered.

The phenomenological descriptions of macroscale friction cannot yet be derived from the fundamental atomic principles, and bridging the gap between different length scales in tribological systems remains an open challenge [15]. Hence, the following sections will be organized into macro-, micro- and nanoscale representing the theoretical understanding governing each scale regime. While our study of the graphene sheet is based on a nanoscale perspective the hypothesizing about application possibilities will eventually draw upon a macroscale perspective as well. Thus, we argue that a brief theoretical introduction to all three major scales is of high interest for a more complete interpretation of the findings in this thesis.

2.1 Macroscale

Our working definition of the *macroscale* is everything on the scale of visible everyday objects, which is usually denoted to the size of millimeters 10^{-3} m and above. Most importantly, we want to make a distinction to the *microscale*, where the prefix indicates the size of micrometers m^{-6} , and hence we essentially assign everything larger than *micro* to the term *macroscale*¹.

2.1.1 Amontons' law

In order to start and keep a solid block moving against a solid surface we must overcome certain frictional forces F_{fric} [1]. The static friction force F_s corresponds to the minimum tangential force required to initiate the sliding while the kinetic friction force F_k corresponds to the tangential force needed to sustain such sliding at steady speed. The work of Leonardo da Vinci (1452–1519), Guillaume Amontons (1663–705) and Charles de Coulomb (1736–1806) all contributed to the empirical law, commonly known as Amontons' law, which serves as a common base for macroscale friction. Amontons' law states that the frictional forces is entirely independent of contact

¹The width of a human hair is on the length scale 10^{-5} to 10^{-4} m which constitute a reasonable boundary between macro- and microscale which fit well with a lower bound of human perception capabilities.

area and sliding velocity. Instead, it relies only on the normal force F_N , acting perpendicular to the surface, and the material specific friction coefficient μ as

$$F_{\text{fric}} = \mu F_N. \quad (2.1)$$

Notice that the term *Normal force* is often used interchangeably with *load* and *normal load* although the latter terms refer to the applied force, pushing the object into the surface, while the first is the corresponding reaction force acting from the surface on the object. These forces are exactly equal in magnitude and hence we will not make a clear distinction in this thesis. On the same note, the frictional force is different from a conventional force which in the Newtonian definition acts on a body from the outside and make it accelerate [17]. Rather than being an independent external force the friction force is an internal *reaction* force opposing the externally applied “sliding” force.

The friction coefficient μ is typically different for the cases of static (μ_s) and kinetic (μ_k) friction, usually both with values lower than one and $\mu_s \geq \mu_k$ in all cases [1, p. 6]. The friction coefficient is taken to be a constant defined by either [17]

$$\mu = \frac{F_{\text{fric}}}{F_N}, \quad (2.2a) \quad \text{or} \quad \mu = \frac{dF_{\text{fric}}}{dF_N}. \quad (2.2b)$$

The first definition (Eq. (2.2a)) requires zero friction at zero load, i.e. $F_{\text{fric}} = 0 \text{ at } F_N = 0$, while the second definition (Eq. (2.2b)) allows for a finite friction force at zero load since the coefficient is instead given by the slope of the F_{fric} versus F_N curve. However, in reality the friction coefficient is not truly a material specific constant as it is often found to vary under different conditions such as humidity or smooth and rough morphologies of the sliding surfaces [17].

Although Amontons’ law has been successful in its description of the majority of rubbing surfaces, involving both dry and lubricated, ductile and brittle and rough and smooth (as long as they are not adhesive) surfaces [17], it has its limitations. It is now known that Eq. (2.1) is not valid over a large range of loads and sliding velocities and that it completely breaks down for atomically smooth surfaces in strongly adhesive contact [17]. The independency of sliding velocity disappears at low velocities as thermal effects becomes important and for high velocities due to inertial effects [1, pp. 5-6]. For the case of static friction, it was later discovered to be dependent on the so-called contact history with increasing friction as the logarithm of time of stationary contact.

In cases where amontons’ law breaks down we might still use the conceptual definition of the friction coefficient as defined by (Eq. (2.2b)). Especially, in the context of achieving negative friction coefficients (in certain load ranges) we would refer to this definition, since (Eq. (2.2a)) would imply a truly unphysical situation of the frictional force acting in the same direction as the sliding motion which would accelerate the object indefinitely².

Due to the empirical foundation of Amontons’ law it does not provide any physical insight into the underlying mechanisms of friction. However, as we will later discuss in more detail, we can understand the overall phenomena of friction through statistical mechanics by the concept of *equipartition of energy* [15]. A system in equilibrium has its kinetic energy uniformly distributed among all its degrees of freedom. When a macroscale object is sliding in a given direction it is clearly not in equilibrium since one of its degrees of freedom carries considerable more kinetic energy. Thus, the system will have a tendency to transfer that kinetic energy to the remaining degrees of freedom as heat. This heat will dissipate to the surroundings and the object will slow down as a result. Hence, we can understand friction simply the tendency of going toward equilibrium energy equipartitioning among many interacting degrees of freedom [15]. From this point of view it is clear that friction is an inevitable part of contact physics, but even though friction cannot be removed altogether, we are still capable of manipulating it in useful ways.

The attentive reader might point out that we have already moved the discussion partly into the microscopic regime as *statistical mechanics* generally aim to explain macroscale behaviour by microscopic interactions. In fact, this highlights the necessity to consider smaller scales in order to achieve a more fundamental understanding of friction.

²You would most likely have a good shot at the Nobel Prize with that paper.

2.2 Microscopic scale

Going from a macro- to microscale perspective, a length scale of order 10^{-6} m, it was realized that most surfaces is in fact rough [18]. The contact between two surfaces consist of numerous smaller contact point, so-called asperities, for which the friction between two opposing surfaces involves interlocking of those asperities as visualized in Fig. 2.1. Small junctions of asperities are formed due to contact pressure and adhesion [3]

In the macroscale perspective of Amonton's law we refer to time- and space-averaged values, i.e. the "apparent" contact area and the average sliding speed [17]. However, microscopically we find the real contact area to be smaller than the macroscale apparent area and the shearing of local microjunctions can happen at large fluctuations or in a stick-slip fashion.

It is generally accepted that friction is caused by two mechanism: mechanical friction and chemical friction [3]. The mechanical friction is the "plowing" of the surface by hard particles or said asperities with an energy loss attributed to deformations of the asperity. While plastic deformations, corresponding to wear, gives rise to an obvious attribution for the energy loss, elastic deformations is also sufficient in explaining energy loss due to phonon excitations. In fact the assumption of plastic deformations has been critizised as this is theorized only to be present in the beginning of surface contact [19]. When machine parts slide against each other for millions of cycle the plastic deformation would only take place in the beginning until the system reaches a steady state with only elastic deformation taking place. The chemical friction arrises from adhesion between microscopic contacting surfaces, with an energy loss attributed to breaking and forming of bonds.

2.2.1 Surface roughness - Asperity theories

Asperity theories are based on the observation that microscopic rough surfaces, with contacting asperities each with a contact area of A_{asp} , will have a true contact area $\sum A_{\text{asp}}$ much smaller than the apparent macroscopic area [3]. The friction force has been shown to be proportional to the true contact area as

$$F_{\text{fric}} = \tau \sum A_{\text{asp}},$$

where τ is an effective shear strength of the contacting bodies. Note that this is compatible with Amontons' law in Eq. (2.1) by having a linear relationship between the real contact area and the applied load. In Fig. 2.1 we see a visualization on how the contact area might intuitively increase with load as the asperity tips is deformed (plastically or elastically) into broader contact points.

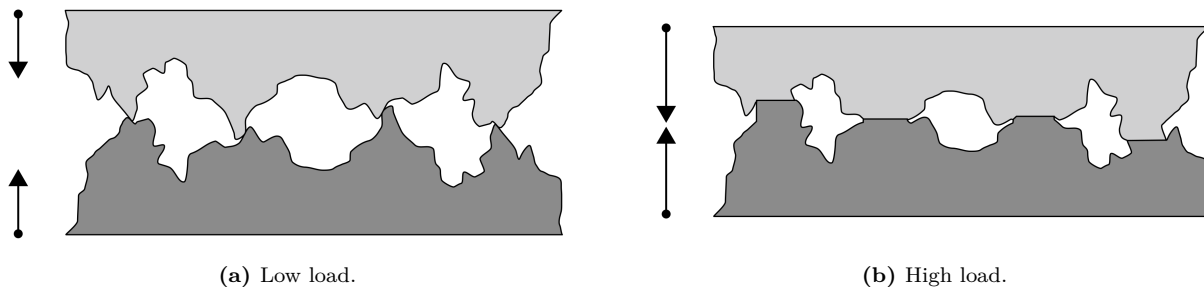


Figure 2.1: Qualitative illustration of the microscopic asperity deformation under increasing load from frame (a) to (b) [20]. While this figure evidently portrays plastic deformation the concept of increased contact area under increased load applies for elastic deformation as well.

Many studies have focused on single asperity contacts to reveal the relationship between the contact area and F_N (13-15 from [18]). By assuming perfectly smooth asperities, with radii of curvature from micrometers all the way down to nanometers, continuum mechanics can be used to predict the deformation of asperities as load is applied. A model for non-adhesive contact between homogenous, isotropic, linear elastic spheres was first developed by Hertz (17 from [18]), which predicted $A_{\text{asp}} \propto F_N^{2/3}$. Later adhesion effects were included in a number of subsequent models, including Maugis-Dugdale theory (18 from [18]), which also predicts a sublinear relationship between A_{asp} and F_N . Thus, the common feature of all single-asperity theories is that A_{asp} is a

sublinear function of F_N , leading to a similar sublinear relationship for $F_{\text{fric}}(F_N)$, which fails to align with the macroscale observations modelled by Amontons' law (eq. (2.1)).

Concurrently with single-asperity studies, roughness contact theories are being developed [18, 8–10, 16] in] to bridge the gap between single asperities and macroscopic contacts [18]. A variety of multi-asperity theories has attempted to combine single asperity mechanics by statistical modelling of the asperity height and spatial distributions [19]. This has led to a partially success in the establishment of a linear relationship between A_{asp} and F_N . Unfortunately, these results are restricted in terms of the magnitude of the load and contact area, where multi-asperity contact models based on the original ideas of Greenwood and Williamson [21] only predicts linearity at vanishing low loads, or Persson [22] which works for more reasonable loads but only up to 10–15 % of the macroscale contact area. However, as the load is further increased all multi-asperity models predict the contact area to fall into the sublinear dependency of normal force as seen for single asperity theories as well [19].

2.3 Nanoscale - Atomic scale

Going from a micro- to a nanoscale, on the order of 10^{-9} m, it has been predicted that continuum mechanics will break down [23] due to the discreteness of individual atoms. Note that atom spacing lies in the domain of a few ångströms Å (10^{-10} m) and thus we take the so-called atomic-scale to be a part of the nanoscale regime. In a numerical study by Mo et al. [18] (considering asperity radii of 5–30 nm) it has been shown that the asperity area A_{asp} , defined by the circumference of the contact zone, is sublinear with F_N . This is accommodated by the observation that not all atoms within the circumference make chemical contact with the substrate. By modelling the real contact area $A_{\text{real}} = N A_{\text{atom}}$, where N is the amount of atoms within the range of chemical interaction and A_{atom} the associated surface area for an atom, they found a consistent linear relationship between friction and the real contact area. Without adhesive forces this lead to a similar linear relationship $F_{\text{fric}} \propto F_N$, while adding van der Waals adhesion to the simulation gave a sublinear relationship, even though the $F_{\text{fric}} \propto A_{\text{real}}$ was maintained. This result emphasizes that the contact area is still expected to play an important role at the nanoscale for asperity theory. It is simply the definition of the contact area that undergoes a change when transitioning from micro- to nanoscale.

However, considering the simulation setup of our numerical study, a flat sheet on a flat substrate, the lack of asperities make it unfounded to rely on asperity theories. Although both numerical and experimental research have been done for so-called nanoflakes sliding on a substrate, no investigation is reported on the dependence of friction force on contact area (to the best of my knowledge at least). One reasonable explanation is that the contact area is already maxed out for atomic smooth surfaces. Since a dependency on normal load is still reported in most nanoflake studies (see section Sec. 2.3.3 or give details on studies here?), this suggests that some other mechanisms are governing friction at this level. Before diving into alternative theoretical approaches to address this issue we point out that exactly this transition, between nanoscale asperities and atomic smooth surfaces, is of outermost importance for the objective of the thesis. By introducing kirigami cuts and stretching the sheet we expect to see an out of plane buckling which induce an ensemble of asperities on the sheet. Hence, we might hypothesize that such a transition will contribute to a significant change in the governing mechanism of friction bridging two (poorly understood) theoretical domains

In the lack of noteworthy structural asperities, friction can instead be modelled as a consequence of the rough potential of the atomic landscape. A series of models builds on this idea by considering different ways for the atoms to interact interatomically, with the moving body, and the substrate. In figure Fig. 2.2 three of the most common 1D models is displayed. The time-honored Prandtl-Tomlinson (PT) model describes a point-like tip sliding over a space-periodic fixed crystalline surface with a harmonic coupling to the moving body. This is analog to that of an experimental cantilever used for Atomic Force Microscopy (see section Sec. 2.3.2.1). Further extensions were added in the Frenkel-Kontorova (FK) model by substituting the tip with a chain of harmonic coupled atoms dragged from the end (I am not sure that the figure is 100% correct by drawing a spring like that), and finally combined in the Frenkel-Kontorova-Tomlinson (FKT) with the addition of a harmonic coupling between the chain and the moving body. In the following we will discuss the FK model as this gives provides a sufficient foundation for the understanding of smooth nanoscale friction.

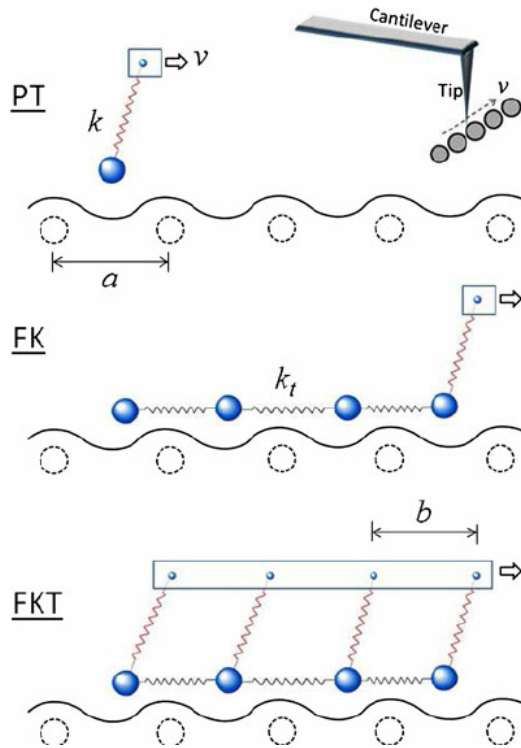


Figure 2.2: Temporary figure from <https://www.researchgate.net/figure/illustrations-of-the-1D-PT-FK-and-FKT-models-Large> fig1_257670317

2.3.1 Frenkel-Kontorova

The standard Frenkel-Kontorova (FK) model consists of a 1D chain of N classical particles of equal mass, representing atoms, interacting via hamornic forces and moving in a sinusoidal potential as sketched in Fig. 2.3 [15]. The hamiltonian is

$$H = \sum_{i=1}^N \left[\frac{p_i^2}{2m} + \frac{1}{2}K(x_{i+1} - x_i - a_c)^2 + \frac{1}{2}U_0 \cos\left(\frac{2\pi x_i}{a_b}\right) \right], \quad (2.3)$$

where the atoms are labelled sequently $i = 1, \dots, N$. The first term $p_i^2/2m$ represents the kinetic energy with momentum p_i and mass m . Often the effetc of inertia are neglected, referred to as the static FK model, while the inclusion, as shown here in Eq. (2.3), is known as the dynamic FK model [24]. The next term describes the harmonic interaction with elastic constant K , nearest neighbour distance $\Delta x = x_{i+1} - x_i$ and corresponding nearest neighbour equilibrium distance a_c . The final term represents the periodic substrate potential (external potential on site) with amplitude U_0 and period a_b . Different boundary choices can be made where both free ends and periodic conditions gives similar results. The choice of fixed ends however makes the chain incapable of sliding.

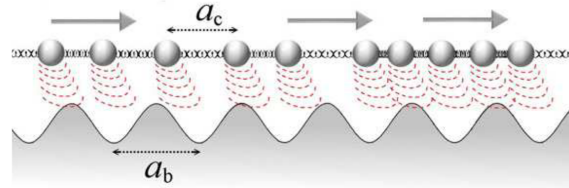


Figure 1. A sketch of the FK model, showing the two competing lengths: the average interparticle spacing and the lattice periodicity of the substrate.

Figure 2.3: [Temporary] figure from [15]

To probe static friction one can apply an external adiabatically increasing force until sliding occurs. This corresponds to the static FK model, and it turns out that the sliding properties are entirely governed by its topological excitations referred to as so-called *kinks* and *antikinks*

2.3.1.1 Commensurability

We can subdivide the frictional behaviour in terms of commensurability, that is, how well the spacing of the atoms match the periodic substrate potential. We describe this by the length ratio $\theta = a_b/a_c = N/M$ where M denotes the number of minemas in the potential (within the length of the chain). A rational number for θ means that we can align the atoms in the chain perfectly with the minemas, without stretching the chain, corresponding to a *commensurate* case. If θ is irrational the chain and substrate cannot fully align without stretching of the chain, and we denote this as being *incommensurate*.

We begin with the simplest commensurate case of $\theta = 1$ where the spacing of the atoms matches perfectly with the substrate potential periodicity, i.e. $a_c = a_b$, $N = M$. The ground state (GS) is the configuration where each atom fits in one of the substrate minemas. By adding an extra atom we would effectively shift over some atoms, away from this ideal state, giving rise to a kink excitation, i.e. two atoms will have to “share” the same potential corrugation as sketched in Fig. 2.5. On the other hand, removing an atom from the chain results in an antikink excitation where one potential corrugation will be left “atomless”. In order to reach a local minimum the kink (antikink) will expand in space over a finite length such that the chain undertakes a local compression (expansion). When applying a tangential force to the chain it is much easier for an excitation to move along the chain than it is for the non-excited atoms since the activation energy ϵ_{PN} for a kink/antikink displacement is systematically smaller (often much smaller) than the potential barrier U_0 . Thus, the motion of kinks (antikinks), i.e. the displacement of extra atoms (atom vacancies), is representing the fundamental mechanism for mass transport. These displacements are responsible for the mobility, diffusivity and conductivity within this model.

In the ideal zero temperature commensurable case with an adiabatical increase in force, all atoms would be put into an accelerating motion as soon as the potential barrier energy is present ($\sim NU_0$ for sufficiently stiff springs). However, in reality any thermal excitation would excite the system before this point is reached resulting in kink-antikink pairs traveling down the chain. For a chain of finite length these often occur at the end of the chain running in opposite direction. As a kink travels down the chain the atoms is advanced by one lattice spacing a_b along the substrate potential. This cascade of kink-antikink excitations is shown in Fig. 2.4

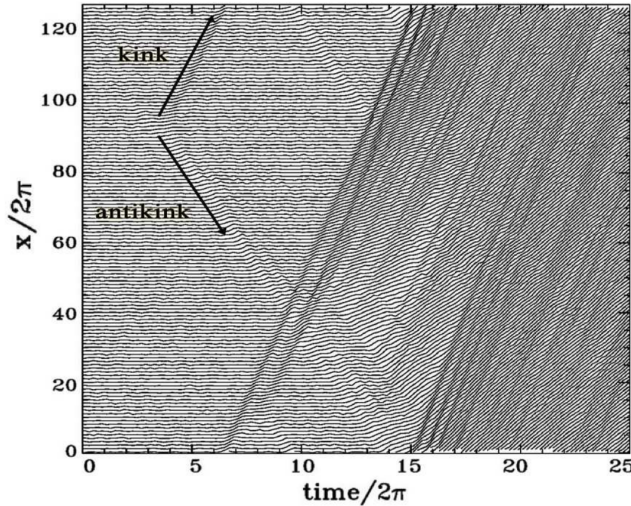


Figure 2. Time dependence of the atomic trajectories for the fully matched ($\theta = 1$) FK model at the (low-temperature) onset of depinning. Motion starts with the nucleation of a kink-antikink pair. The kink and the antikink depart in opposite directions cross the periodic boundary conditions, and collide quasielastically. A second kink-antikink pair forms in the wake of the initial kink. Further kink-antikink pairs are generated, with an avalanche-like increase of the kink-antikink concentration, eventually leading to a sliding state. Adapted from Ref. [21], Copyright (1997) by The American Physical Society.

Figure 2.4: Temporary figure from [15]

For the 2D case where an island (or flake) is deposited on a surface, in our case the graphene sheet on the Si substrate, we generally also expect the sliding to be initiated by kink-antikink pairs at the boundary.

For the case of incommensurability, i.e. $\theta = a_b/a_c$ is irrational, the GS is characterized by a sort of ‘‘staircase’’ deformation. That is, the chain will exhibit regular periods of regions where the chain is slightly compressed (expanded) to match the substrate potential, separated by kinks (antikinks), where the increased stress is eventually released through a localized expansion (compression) as illustrated in Fig. 2.5 Go through this last part again. Even though this is what the source says I'm not quite sure I understand why it is not opposite ‘‘...released through a localized compression (expansion)’’?



Figure 2.5: Temporary figure from [urlhttp://www.iop.kiev.ua/~obraun/myreprints/surveyfk.pdf](http://www.iop.kiev.ua/~obraun/myreprints/surveyfk.pdf) p. 14. Incommensurable case ($\theta = ?$) where atoms sit closer than otherwise dictated by the substrate potential for which this regularly result in a kink here seen as the presence of two atoms closely together in one of the potential corrugations.

The incommensurable FK model contains a critical elastic constant K_c , such that for $K > K_c$ the static friction F_s drops to zero, making the chain able to initiate a slide at no energy cost, while the low-velocity kinetic friction is dramatically reduced. This can be explained by the fact that the displacement occurring in the incommensurable case will yield just as many atoms climbing up a corrugation as there are atoms climbing down. For a big (infinite) chain this will exactly balance the forces making it non-resistant to sliding. Generally, incommensurability guarantees that the total energy (at $T = 0$) is independent of the relative position to the potential. However, when sliding freely a single atom will eventually occupy a maximum of the potential. When increasing the potential magnitude U_0 or softening the chain stiffness, lowering K , the possibility to occupy such

a maximum disappears. This marks the so-called Aubry transition at the critical elastic constant $K = K_c(U_0, \theta)$ where the chain goes from a free sliding to a *pinned state* with a nonzero static friction. K_c is a discontinuous function of the ratio θ , due to the reliance on irrational numbers for incommensurability. The minimal value $K_c \simeq 1.0291926$ in units $[2U_0(\pi/a_b)^2]$ is achieved for the golden-mean ratio $\theta = (1 + \sqrt{5}/2)$. Notice that the pinning is provided despite translational invariance due to the inaccessibility to move past the energy barrier which act as a dynamical constraint. The Aubry transition can be investigated as a first-order phase transition for which power laws can be defined for the order parameter. This is beyond the scope of this thesis as we merely are going to point to the FK model for the understanding of stick-slip behaviour and the concept of commensurability.

The phenomena of non-pinned configurations is named *superlubricity* in tribological context. Despite the misleading name this refers to the case where the static friction is zero while the kinetic friction is nonzero but reduced. For the case of a 2D sheet it is possible to alter the commensurability by changing the orientation of the sheet relative to the substrate. This has been shown for a graphene flake sliding over a graphite surface (multiple layers of graphene) [25] as shown in Fig. 2.6. We clearly see that friction changes as a function of orientation angles with only two spikes of considerable friction force.

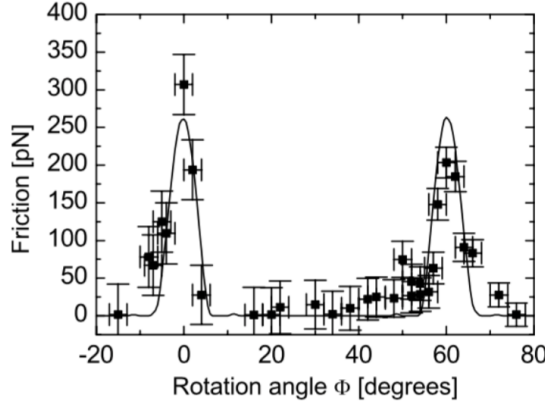


Fig. 6. Average friction force versus rotation angle Φ of the graphite sample around an axis normal to the sample surface. Two narrow peaks of high friction are observed at 0° and 61° , respectively. Between these peaks a wide angular range with ultra-low friction, close the detection limit of the instrument, is found. The first peak has a maximum friction force of 306 ± 40 pN, and the second peak has a maximum of 203 ± 20 pN. The curve through the data points shows results from a Tomlinson model for a symmetric 96-atom graphite flake sliding over the graphite surface (for details about the calculation see [39]).

Figure 2.6: **Temporary** figure from [25] showing superlubricity for incommensurable orientations between graphene and graphite. **temporary**

2.3.1.2 Kinetic friction

In the FK model the kinetic friction is primarily caused by resonance between the sliding induced vibrations and phonon modes in the chain [24]. The specific dynamics is found to be highly model and dimension specific, and even for the 1D case this is rather complex. However, we make a simplified analysis of the 1D case to showcase the reasoning behind the phenomena.

When all atoms are sliding rigidly with center of mass velocity v_{CM} the atoms will pass the potential maxima with the so-called *washboard frequency* $\Omega = 2\pi v_{CM}/a_b$. For a weak coupling between the chain and the potential we can use the zero potential case as an approximation for which the known dispersion relation for the

1D harmonic chain is given [Kittel (add to bibliography)]

$$\omega_k = \sqrt{\frac{4K}{m}} \left| \sin\left(\frac{k}{2}\right) \right|,$$

where ω_k is the phonon frequency and $k = 2\pi i/N$ the wavenumber with $i \in [N/2, N/2]$. Resonance will occur when the washboard frequency Ω is close to the frequency of the phonon modes ω_q in the chain with wavenumber $q = 2\pi a_c/a_b = 2\pi\theta^{-1}$ or its harmonics nq for $n = 1, 2, 3, \dots$ [26]. Thus, we can approximate the resonance COM speed as

$$\begin{aligned} n\Omega &\sim \omega_{nq} \\ n\frac{2\pi v_{CM}}{a_b} &\sim \sqrt{\frac{4K}{m}} \left| \sin\left(\frac{2n\pi\theta^{-1}}{2}\right) \right| \\ v_{CM} &\sim \frac{\sin(n\pi\theta^{-1})}{n\pi} \sqrt{\frac{Ka_b^2}{m}}. \end{aligned}$$

When the chain slides with a velocity around resonance speed, the washboard frequency can excite acoustic phonons which will dissipate to other phonon modes as well. At zero temperature the energy will transform back and forth between internal degrees of freedom and center of mass movement of the chain. Hence, at zero temperature this is in fact theorized to speed up the translational decay. However, for the more realistic case of a non-zero temperature the substrate serves as a thermostat, for which energy will dissipate from the chain to the substrate degrees of freedom, giving rise to kinetic friction. This suggests that certain sliding speeds will exhibit relatively big kinetic friction while others will be subject to extremely low kinetic friction. Simulations of concentric nanotubes in relative motion (telescopic sliding) have revealed the occurrence of certain velocities at which the friction is enhanced, corresponding to the washboard frequency of the system [15]. The friction response was observed to be highly non-linear as the resonance velocities were approached.

A common way to model the non-zero temperature case is by the use of a Langevin thermostat, which models the dissipation of heat by adding a viscous damping force and thermal fluctuations by the addition of Gaussian random forces with variance proportional to the temperature (This is covered in more details in section ??). In combination, this gives rise to a kinetic friction that is both velocity and temperature dependent.

By extending the FK model into 2D [24] it can be shown numerically that the friction coefficient generally increases with increasing velocity and temperature respectively, although the specific of the trend is highly sensitive to model parameters.

2.3.1.3 Temperature dependence

Might find something interesting here [27] or [28].

2.3.1.4 Smooth sliding

Find a suitable place to introduce smooth sliding. Above certain velocities the stick-slip motion disappear. [1, p. 142-ish]

2.3.2 Experimental procedures

Experimentally, the study of nanoscale friction is challenging due to the low forces on the scale of nano-newtons along with difficulties of mapping nanoscale topography [1, p. ?]. Numerically, simulations provide full transparency regarding atomic-scale structures and sampling of forces, velocities and temperature. Of course, this comes with a possible cost of realism as we will address later (do we actually). In order to compare numerical and experimental results, the experimental procedures are often mirrored in simulations. Thus, it is relevant to address the most common experimental techniques before designing a simulation.

2.3.2.1 Scanning Probe Microscopy

Scanning probe microscopy (SPM) includes a variety of experimental methods which is used to examine surfaces with atomic resolution [29, p. 6-?]. This was originally developed for surface topography imaging, but today

it plays a crucial role in nanoscale science as it is used for probe-sampling regarding tribological, electronic, magnetic, biological and chemical character. The family of methods involving the measurement of forces is generally referred to as *scanning force microscopies* (SFM) or for friction purposes *friction force microscopes* (FFM).

One such method arose from the *atomic force microscope*, which consist of a sharp micro-fabricated tip attached to a cantilever force sensor, usually with a sensitivity below 1 nN. The force is measured by recording the bending of the cantilever, either as a change in electrical conduction or more commonly, by a light beam reflected from the back of the cantilever into a photodetector [1]. By adjusting the tip-sample height to keep a constant normal force while scanning across the surface this can be used to produce a surface topography map. By tapping the material (dynamic force microscopy) with sinusoidally vibrated tip the effects from friction and other disturbing forces can be minimized in order to produce an even clearer image (include example, preferable showing the surface structure of graphene). However, when scanning perpendicularly to the cantilever axis, one is also able to measure the frictional force as torsion of the cantilever. By having four quadrants in the photodetector (as shown in figure Fig. 2.7), one can simultaneously measure the normal force and friction force as the probes scans across the surface.

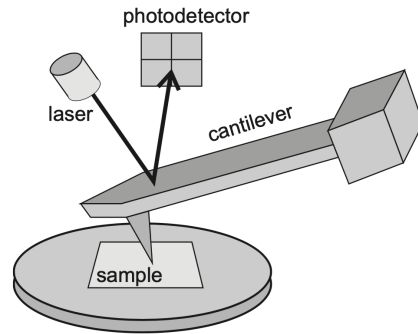


Figure 17.1 Schematic diagram of a beam-deflection atomic force microscope.

Figure 2.7: Temporary figure from [1, p. 184]

AFM can also be used to drag a nanoflake across the substrate as done by Dienwiebel et al. [25], where a graphene flake was attached to a FFM tip and dragged across graphite. However, this makes the normal loading concentrated to a single point on the flake.

2.3.2.2 Surface Force Apparatus (SFA)

I think this refers to having two interfaces sliding against each other with (optionally I think) lubrication between. This is often mirrored in MD simulations and often experimental results refer to this. So it might be worth saying a few words about, but I'm not sure yet.

2.3.3 (summary of) Expected frictional properties

The structural setup of our simulation is most reminiscent a graphene flake sliding on a substrate. This has been studied numerically in molecular dynamic simulations by Zhu and Li [30, p. 2018] for a graphene flake on a gold substrate and by Zhang et al. [31](2019) on a diamond substrate, and in a tight-binding simulation by Bonelli et al. [32](2009) for graphene on graphite. Experimental studies of a graphene flake attached to an AFM is done by Dienwiebel et al. [25, p. 2005] and Feng et al. [33, p. 2013] sliding on graphite, but these are mainly concerned with superlubricity due to flake orientation commensurability.

In our study we simulate a graphene flake on a silicon substrate which deviates slightly from the above-mentioned references by having a different material combination. Additionally, the normal force is only applied to the ends of the sheet which might have an important effect. Obviously stretching and cutting the sheet will separate our study dramatically from the references, but we aim to compare the frictional properties to the references before applying stretch or cuts.

In the following we summarize the qualitative expectations for the nanofriction behaviour for the unstretched and non-cut graphene sheet.

2.3.3.1 Qualitatively

1. **Stick slip:** Generally we expect to observe periodic stick-slip motion with a period matching the lattice constant(s) involved [18]. This was both present in the MD simulations [30], [31] and in the experiment by [25]. In AFM and SFA experiments, the stick-slip motion tends to transition into smooth sliding when the speed exceeds $\sim 1 \mu\text{m/s}$ while in MD modelling the same transition is observed in the $\sim 1 \text{ m/s}$ region [15]. Since we use a sliding speed of 20 m/s we might transition into smooth sliding. This 6 order of magnitude discrepancy has been largely discussed in connection to simplifying assumptions in MD simulations. Bonelli et al. [32] found that the stick-slip behaviour was present when the cantilever-tip-flake coupling was done with a relatively soft springs in contrast to hard springs which inhibited it.
2. **Static friction:** As highlighted in the FK model static friction will be sensitive to commensurability, which will additionally be affected by flake size. Reguzzoni and Righi [34] have shown that the effective commensurability will increase drastically below a critical flake radius on the order of 10 Å. Macroscopically we expect to see a logarithmic increase in static friction with contact time before sliding [35], and hence due to the short time-span of the static contact before dragging, it is not obvious to determine whether a significant static friction peak will be found. Also, the static friction best asserted by increasing the tangential sliding force slowly which is not the case in our simulation, especially considering that we are going to move the sheet rigidly (infinite spring constant) without any slack of a soft spring. Edge related origin of the pinning effects suggest that static friction can increase with sheet size up to a factor $A \propto A^{1/2}$, but this is also reported to be specific of the contact shape [15].
3. **Orientation (friction anisotropy):** As predicted by the FK model and confirmed both numerically [30], [31] and experimentally [25], [33] we expect a dependence of friction force on orientation due to changing commensurability. Zhu and Li [30] (gold substrate) reported the highest friction when sliding along the armchair direction, while Zhang et al. [31] (diamond substrate) found the zigzag-direction to give the highest friction force (also the most evident stick-slip behaviour in this direction).

By consulting with the most related numerical and experimental studies, while also considering the theoretical gap between smooth atomic contact and asperity theory, we have summarized an evaluation of the most important quantitative trends expected from our numerical results in ??.

Table 2.1: Quantitative nano friction dependence on various variables. work in progress.

Variable	Dependency	Numerical studies	Experimental
Normal force F_N	$F_{\text{fric}} \propto F_N^\alpha$ $\alpha \leq 1$	Zhang et al. [31] finds a seemingly linear relationship $F_{\text{fric}} \propto F_N$ while Bonelli et al. [32] reports a sublinear relationship. The latter corresponds with that of nanosasperity simulations where Mo et al. [18], using an amorphous carbon tip on a diamond sample, also found a sublinear relationship when including adhesion and linear without adhesion.	Experimentally rather different trends have been observed, although the majority agree on increasing friction with increasing load [1, p. 200]. For the graphebne flake Dienwiebel et al. [25] found a seemingly non-dependent relationship while Feng et al. [33] did not report on this. FFM analog to the single asperity setup have yielded both linear relationship [17] (silicon tip on gold) while Schwarz et al. [36] found that FFM with well-defined spherical tips matched with theoretical results (DMT, elastic spheres pressed together [1, p. 200]), yielding a power law $F_{\text{fric}} = F_N^{2/3}$.
Velocity v	$F_{\text{fric}} \propto \ln v$ (exp.) or $F_{\text{fric}} \propto v$ (num.)	Studies of gold clusters on graphite suggest that friction is viscous, i.e. proportional to velocity [15].	Logarithmic velocity dependence of friction has been measured for nanotip friction [1, p. 201] associated to thermal activation and possibly the time available to form bond between the tip and the substrate. At higher velocities thermally activated processes are less important and friction becomes independent of velocity. This has been observed for Si tips and diamond, graphite and amorphous carbon surfaces with scan velocities above $1 \mu\text{s}$.
Temperature T	Either increase (MD) or decrease as $F_{\text{fric}} \propto \exp(1/T)$ (experimental)	Zhang et al. [31] found simply that friction increased with temperature. The [15] gold cluster on graphite study (get reference) found that the temperature dependence was dependent on velocity regime. Low speed (diffusive) friction decreases upon heating while high speed (ballistic) friction rises with temperature.	Zhao et al. [27] found $F_{\text{fric}} \propto \exp(1/T)$.
Real contact area A	$F_{\text{fric}} \propto A$	Mo et al. [18] found that $F_{\text{fric}} \propto A$ where A is the real contact area defined by atoms within chemical range. This is not studied for the case of a nanoflake where the contact area is presumably rather constant.	

Part II

Simulations

Appendices

Appendix A

Appendix B

Appendix C

Bibliography

- ¹E. Gnecco and E. Meyer, *Elements of friction theory and nanotribology* (Cambridge University Press, 2015).
- ²Bhusnur, “Introduction”, in *Introduction to tribology* (John Wiley & Sons, Ltd, 2013) Chap. 1, 1–?
- ³H.-J. Kim and D.-E. Kim, “Nano-scale friction: a review”, *International Journal of Precision Engineering and Manufacturing* **10**, 141–151 (2009).
- ⁴K. Holmberg and A. Erdemir, “Influence of tribology on global energy consumption, costs and emissions”, *Friction* **5**, 263–284 (2017).
- ⁵B. Bhushan, “Gecko feet: natural hairy attachment systems for smart adhesion – mechanism, modeling and development of bio-inspired materials”, in *Nanotribology and nanomechanics: an introduction* (Springer Berlin Heidelberg, Berlin, Heidelberg, 2008), pp. 1073–1134.
- ⁶P. Z. Hanakata, E. D. Cubuk, D. K. Campbell, and H. S. Park, “Accelerated search and design of stretchable graphene kirigami using machine learning”, *Phys. Rev. Lett.* **121**, 255304 (2018).
- ⁷P. Z. Hanakata, E. D. Cubuk, D. K. Campbell, and H. S. Park, “Forward and inverse design of kirigami via supervised autoencoder”, *Phys. Rev. Res.* **2**, 042006 (2020).
- ⁸L.-K. Wan, Y.-X. Xue, J.-W. Jiang, and H. S. Park, “Machine learning accelerated search of the strongest graphene/h-bn interface with designed fracture properties”, *Journal of Applied Physics* **133**, 024302 (2023).
- ⁹Y. Mao, Q. He, and X. Zhao, “Designing complex architectured materials with generative adversarial networks”, *Science Advances* **6**, eaaz4169 (2020).
- ¹⁰Z. Yang, C.-H. Yu, and M. J. Buehler, “Deep learning model to predict complex stress and strain fields in hierarchical composites”, *Science Advances* **7**, eabd7416 (2021).
- ¹¹A. E. Forte, P. Z. Hanakata, L. Jin, E. Zari, A. Zareei, M. C. Fernandes, L. Sumner, J. Alvarez, and K. Bertoldi, “Inverse design of inflatable soft membranes through machine learning”, *Advanced Functional Materials* **32**, 2111610 (2022).
- ¹²S. Chen, J. Chen, X. Zhang, Z.-Y. Li, and J. Li, “Kirigami/origami: unfolding the new regime of advanced 3D microfabrication/nanofabrication with “folding””, *Light: Science & Applications* **9**, 75 (2020).
- ¹³Z. Deng, A. Smolyanitsky, Q. Li, X.-Q. Feng, and R. J. Cannara, “Adhesion-dependent negative friction coefficient on chemically modified graphite at the nanoscale”, *Nature Materials* **11**, 1032–1037 (2012).
- ¹⁴R. W. Liefferink, B. Weber, C. Coulais, and D. Bonn, “Geometric control of sliding friction”, *Extreme Mechanics Letters* **49**, 101475 (2021).
- ¹⁵N Manini, O. M. Braun, E Tosatti, R Guerra, and A Vanossi, “Friction and nonlinear dynamics”, *Journal of Physics: Condensed Matter* **28**, 293001 (2016).
- ¹⁶B. Bhushan and A. V. Kulkarni, “Effect of normal load on microscale friction measurements”, *Thin Solid Films* **278**, 49–56 (1996).
- ¹⁷J. Gao, W. D. Luedtke, D. Gourdon, M. Ruths, J. N. Israelachvili, and U. Landman, “Frictional forces and amontons’ law: from the molecular to the macroscopic scale”, *The Journal of Physical Chemistry B* **108**, Publisher: American Chemical Society, 3410–3425 (2004).
- ¹⁸Y. Mo, K. T. Turner, and I. Szlufarska, “Friction laws at the nanoscale”, *Nature* **457**, 1116–1119 (2009).
- ¹⁹G. Carbone and F. Bottiglione, “Asperity contact theories: do they predict linearity between contact area and load?”, *Journal of the Mechanics and Physics of Solids* **56**, 2555–2572 (2008).

- ²⁰W. Commons, *File:asperities.svg — wikimedia commons, the free media repository*, [Online; accessed 3-February-2023], 2022.
- ²¹J. A. Greenwood and J. B. P. Williamson, *Contact of nominally flat surfaces*, en, 1966.
- ²²B. N. J. Persson, “Theory of rubber friction and contact mechanics”, *The Journal of Chemical Physics* **115**, 3840–3861 (2001).
- ²³B. Luan and M. O. Robbins, “The breakdown of continuum models for mechanical contacts”, *Nature* **435**, 929–932 (2005).
- ²⁴J. Norell, A. Fasolino, and A. Wijn, “Emergent friction in two-dimensional frenkel-kontorova models”, *Physical Review E* **94**, 10.1103/PhysRevE.94.023001 (2016).
- ²⁵M. Dienwiebel, N. Pradeep, G. S. Verhoeven, H. W. Zandbergen, and J. W. Frenken, “Model experiments of superlubricity of graphite”, *Surface Science* **576**, 197–211 (2005).
- ²⁶J. A. van den Ende, A. S. de Wijn, and A. Fasolino, “The effect of temperature and velocity on superlubricity”, *Journal of Physics: Condensed Matter* **24**, 445009 (2012).
- ²⁷X. Zhao, M. Hamilton, W. G. Sawyer, and S. S. Perry, “Thermally activated friction”, *Tribology Letters* **27**, 113–117 (2007).
- ²⁸S. Y. Krylov, K. B. Jinesh, H. Valk, M. Dienwiebel, and J. W. M. Frenken, “Thermally induced suppression of friction at the atomic scale”, *Phys. Rev. E* **71**, 065101 (2005).
- ²⁹B. Bhushan, “Nanotribology and nanomechanics”, *Wear* **259**, 15th International Conference on Wear of Materials, 1–? (2005).
- ³⁰P. Zhu and R. Li, “Study of nanoscale friction behaviors of graphene on gold substrates using molecular dynamics”, *Nanoscale Research Letters* **13**, 34 (2018).
- ³¹J. Zhang, E. Osloub, F. Siddiqui, W. Zhang, T. Ragab, and C. Basaran, “Anisotropy of graphene nanoflake–diamond interface frictional properties”, *Materials* **12**, 10.3390/ma12091425 (2019).
- ³²F. Bonelli, N. Manini, E. Cadelano, and L. Colombo, “Atomistic simulations of the sliding friction of graphene flakes”, *The European Physical Journal B* **70**, 449–459 (2009).
- ³³X. Feng, S. Kwon, J. Y. Park, and M. Salmeron, “Superlubric sliding of graphene nanoflakes on graphene”, *ACS Nano* **7**, Publisher: American Chemical Society, 1718–1724 (2013).
- ³⁴M. Reguzzoni and M. C. Righi, “Size dependence of static friction between solid clusters and substrates”, *Phys. Rev. B* **85**, 201412 (2012).
- ³⁵J. H. Dieterich, “Time-dependent friction in rocks”, *Journal of Geophysical Research (1896-1977)* **77**, 3690–3697 (1972).
- ³⁶U. D. Schwarz, O. Zwörner, P. Köster, and R. Wiesendanger, “Quantitative analysis of the frictional properties of solid materials at low loads. i. carbon compounds”, *Phys. Rev. B* **56**, 6987–6996 (1997).